



**HAL**  
open science

## **Motion of a two- degree-of-freedom structure in the presence of a fluid-elastic force**

Grégory Turbelin, Rene Jean Gibert, Gérard Porcher

### ► **To cite this version:**

Grégory Turbelin, Rene Jean Gibert, Gérard Porcher. Motion of a two- degree-of-freedom structure in the presence of a fluid-elastic force. ASME Pressure Vessels & Piping Conference, 1996. <hal-02367672>

**HAL Id: hal-02367672**

**<https://hal.science/hal-02367672v1>**

Submitted on 18 Nov 2019

**HAL** is a multi-disciplinary open access archive for the deposit and dissemination of scientific research documents, whether they are published or not. The documents may come from teaching and research institutions in France or abroad, or from public or private research centers.

L'archive ouverte pluridisciplinaire **HAL**, est destinée au dépôt et à la diffusion de documents scientifiques de niveau recherche, publiés ou non, émanant des établissements d'enseignement et de recherche français ou étrangers, des laboratoires publics ou privés.



HAL Authorization

---

---

# MOTION OF A TWO-DEGREE-OF-FREEDOM STRUCTURE IN THE PRESENCE OF A FLUIDELASTIC FORCE

Grégory TURBELIN

Gérard PORCHER

René-Jean GIBERT

CEMIF

Université d'Evry Val d'Essonne  
France

## ABSTRACT

The fluidelastic force induced by a confined flow in a bidimensionnal flow channel, has been determined by using a method which takes into account the dissipative effects by a linearising of the pressure losses considered as boundary conditions. This force has been used to study the stability of a two-degree-of-freedom structure for several boundary conditions.

The motion equation of the system can be solved with an iterative method, and a parametric study has been carried out. The results obtained show the appearance of a flutter instability which has been largely influenced by the position and the value of the pressure losses.

## INTRODUCTION

A fluid flowing through a structure induces fluidelastic forces which are of practical importance because of their destructive effects : the motion of the structure may be coupled with the force exerted by the flow and a dynamic instability may causes fatigue failure. The fluidelastic instabilities are characterized by large-amplitude vibrations and are assumed to be due to energizing transfers from the flow to the structure. These instabilities are often induced by confined flows, because the more confined is the flow, the stonger is the fluidelastic force. Furthermore, these instabilities are largely influenced by the boundary conditions and by the dissipative effects. Several methods have been developed to determine the fluidelastic forces : an approach consists of a potential flow description, see Paidoussis (1966), Mateescu (1985), De Langre (1990),

Porcher (1994). Another approach consists of taking into account the dissipative effects and the boundary-conditions influences, see Miller (1970), Spurr and Hobson (1984), Mulcahy (1988), Inada and Hayama (1988), Porcher (1994). One of these approach is the model in which the pressure losses are linearized and considered as boundary conditions. This method has been generalized to multi-degree-of-freedom structures by Porcher (1994).

In this paper, we study the stability of a two-degree-of-freedom structure excited by a fluidelastic force induced by a confined flow. The force is determined by using the results obtained by Porcher (1994). The motion equation of the coupled fluid-structure system are solved with an iterative method and a parametric study has been carried out to show how the pressure losses affect the stability of the system.

## THE TWO-DEGREE-OF-FREEDOM STRUCTURE

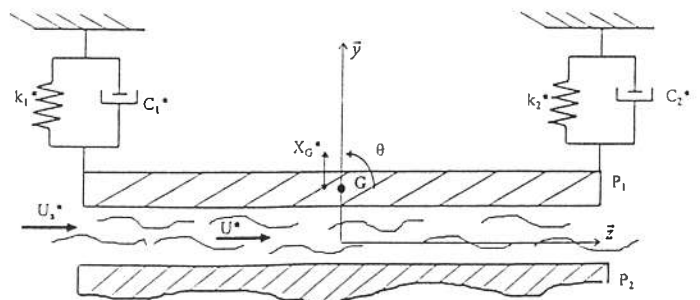


Figure 1 : two-degree-of-freedom structural model

The fluid-structure system is a bidimensionnal flow channel as shown in Figure 1.  $P_1$  is assumed to have two degree of freedom : a vertical translation in direction  $\vec{y}$ , denoted by  $X_G^*$ , and a rotation in direction  $\vec{x}$ , denoted by  $\theta$ .  $P_2$  is a motionless plane. The area between  $P_1$  and  $P_2$  is the fluid-area,  $\mathcal{D}$ . The fluid is incompressible and flows through the fluid-area,  $\mathcal{D}$ , in direction  $\vec{z}$ .  $P_1$  and  $P_2$  are parallel when the fluid is motionless.

### The structural parameters

A unit span of the structure  $P_1$  has mass  $m^* = 156Kg/m$ . The structural stiffness and the damping are provided by springs and shock absorbers, the damping constants are  $C_1^* = C_2^* = 4400 Ns/m^2$ , the spring constants are  $k_1^* = k_2^* = 4.10^6 N/m^2$ .

The structure has length  $2L^* = 0.5m$  and height  $H^* = 10^{-2}m$ , the fitness ratio is  $\epsilon = \frac{L^*}{H^*} = 25$ . The fluid density is  $\rho^* = 1000Kg/m^3$ .

When the fluid is motionless, the natural frequency and the reduced damping are  $f_1^* = 29Hz$  and  $\xi_1 = 0.01$ , for the translational mode, and  $f_2^* = 91.3Hz$  and  $\xi_2 = 0.03$ , for the rotational mode.

### The motion equation

The dimensionless motion equations (variables without asterisk, see appendix) of the system shown in Figure 1, can be put in a matrix form :

$$[M_s]\ddot{X} + [A_s]\dot{X} + [R_s]X = F \quad (1)$$

where  $X = {}^t(X_G; \theta)$ ;  $[M_s], [A_s], [R_s]$  are the dimensionless mass, damping, stiffness matrix of the structure  $P_1$ , written in appendix (table 1);  $F$  is the fluidelastic force.

### The fluidelastic force

To determine the fluidelastic force, the pressure induced by the flow on the structure has to be determined by solving the momentum equation and the continuity equation. These equations have been rendered non-dimensionnal, linearized, expressed in terms of modal components and solved for different boundary conditions by Porcher (1994, 1995). The generalized forces, for an harmonic motion, can be expressed in a matrix form, as shown in appendix (table 2) :

$$F = \{[M_a]\omega^2 - i[A_a(\omega)]\omega - [R_a(\omega)]\}X \quad (2)$$

where  $\omega$  is the reduced frequency,  $i = \sqrt{-1}$  and  $X = {}^t(X_G; \theta)$

The equation (1) becomes :

$$\{-[M_a + M_s]\omega^2 + i[A_a(\omega) + A_s]\omega + [R_a(\omega) + R_s]\}X = 0$$

## THE SOLVING METHOD

### The eigenvalues problem

In order to study the stability of the system, the dimensionless reduced frequencies, of the fluid-structure system, have to be determined by solving the motion equation :

let  $Y$  be defined by :

$$X = \begin{pmatrix} X_G \\ \theta \end{pmatrix}; \dot{X} = \begin{pmatrix} \dot{X}_G \\ \dot{\theta} \end{pmatrix}; Y = \begin{pmatrix} X \\ \dot{X} \end{pmatrix}$$

with this substitution the second-order motion equation becomes a first-order equation :

$$(i\omega C + D)Y = 0 \quad (3)$$

with  $C$  and  $D$   $4 \times 4$ -matrix

$$C = \begin{pmatrix} A & 0 \\ 0 & M \end{pmatrix}; D = \begin{pmatrix} 0 & -A \\ R & A \end{pmatrix}$$

where :  $M = [M_s] + [M_a]$ ;  $A = [A_s] + [A_a(\omega)]$ ;  $R = [R_s] + [R_a(\omega)]$

let  $i\omega = -\lambda$ , equation (3) is substituted into equation (4) :

$$(D - \lambda C)Y = 0 \quad (4)$$

The eigenvalues problem (4) has four solutions,  $\lambda_j$  ( $j = \{1, 2, 3, 4\}$ ), so four reduced frequencies,  $\omega_j = i\lambda_j$ , are obtained. The reduced frequencies of the system,  $\omega_n$  ( $n = \{1, 2\}$ ), are the two solutions with positive real parts.

### The iterative method

Because of the dependance of  $\omega$  upon the dimensional upstream velocity  $U_a^*$  and because of the dependance of the matrix  $[A_a]$  and  $[R_a]$  upon  $\omega$ , an iterative method has been developed to determine  $\omega$  as a function of  $U_a^*$  :

\* a velocity step,  $\Delta U_a$ , is chosen. The reduced frequencies are calculated for the velocities defined by  $U_{a^{k+1}}^* = U_{a^k}^* + \Delta U_a$  and for several corrector iterations, \* at a given velocity  $U_{a^k}^*$ , the values of the reduced frequencies,  $\omega_{n^k}^*$ , corresponding to that velocity are obtained by solving the equation (4).

Next :

- the matrix  $[A_a(\omega)]$  and  $[R_a(\omega)]$  are calculated for  $\omega = \omega_{n_1}^k$ ,
- by using the preceding method, new reduced frequencies  $\omega_{n_2}^k$  are calculated,
- if  $|\omega_{n_2}^k - \omega_{n_1}^k| \leq \delta$ , the solutions converge ( $\delta$  is a given parameter function of the desired degree of convergence),
- if  $|\omega_{n_2}^k - \omega_{n_1}^k| \geq \delta$ , the procedure is repeated until  $|\omega_{n_{j+1}}^k - \omega_{n_j}^k| \leq \delta$

\* When the solutions converge, the problem is solved for another velocity  $U_{a^{k+1}}^* = U_{a^k}^* + \Delta U_a$ .

### Stability analysis

A complex reduced frequency  $\omega$ , solution of the motion equation, can be expressed as follows :

$$\omega = \omega_0 \sqrt{1 - \xi^2} + i\xi\omega_0 \quad (5)$$

The stability can be directly determined from the natural reduced frequency,  $\omega_0$ , and from the reduced damping,  $\xi$ , of the fluid-structure system :

- buckling instability is defined for  $\omega_0 = |\omega| = 0$
- flutter instability is defined for  $\xi = \frac{Im(\omega)}{|\omega|} \leq 0$

By determining  $\omega$  as a function of the flow velocity,  $U_a^*$ , the critical velocity (i.e. the velocity which causes the structure to instability) can be predicted.

### PARAMETRIC STUDY

We have performed a flow-induced-vibration predictive analysis to study the influence of the position and of the values of the pressure losses on the appearance of flutter instabilities for the structure described in Figure 1. Three boundary conditions have been chosen :

- upstream pressure loss,
- downstream pressure loss,
- both upstream and downstream pressure losses.

Our aim is first to compare the stability of the three cases and second to show that for the unstable cases, the critical velocity is a function of the values of the pressure loss factor. The reduced damping,  $\xi$ , is obtained as a function of the upstream velocity,  $U_a^*$ , by using the iterative method exposed above. The critical value of the velocity is obtained from the plot of this function.

### Upstream pressure loss

The dependance of  $\xi$  upon  $U_a^*$  and upon the upstream pressure loss factor  $K_1$  is shown on Figure 2 for the translational mode and on Figure 3 for the rotational mode.

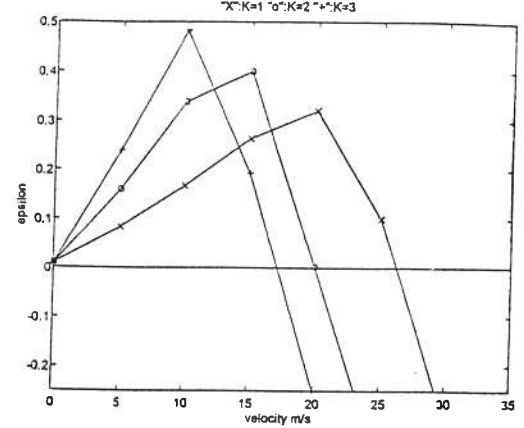


Figure 2 : Translational mode,  $\xi$  as a function of  $U_a^*$  and as a function of  $K_1$

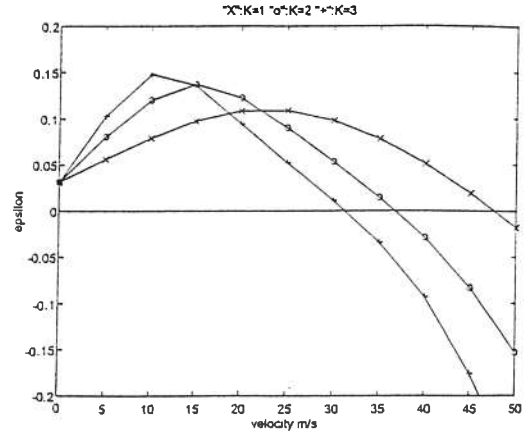


Figure 3 : rotational mode,  $\xi$  as a function of  $U_a^*$  and as a function of  $K_1$

For a given value of  $K_1$ , note that the reduced damping increases with the velocity and abruptly goes to zero and becomes negative. At a certain critical flow velocity the structure becomes fluidelastically unstable : the negative damping mechanism extracts energy from the fluid flow and inputs energy into the structure to encourage, initially, vibration, and ultimately flutter. The critical flutter velocity is identified where the plots,  $\xi=0$  and  $\xi$  vs.  $U_a^*$ , cross. (It should be appreciated that the instabilities are as sudden as the ones observed on fluid conveying structures).

These results agree with the stability analysis performed by Porcher (1994) and with the results obtained by Miller (1970).

### Both upstream and downstream pressure losses

The dependance of  $\xi$  upon  $U_a^*$  and upon the downstream pressure loss factors  $K_1$  and  $K_2$ , is shown on Figure 7 for the translational mode and on Figure 8 for the rotational mode. On these figures  $K_1=2$  and  $K_2$  increases.

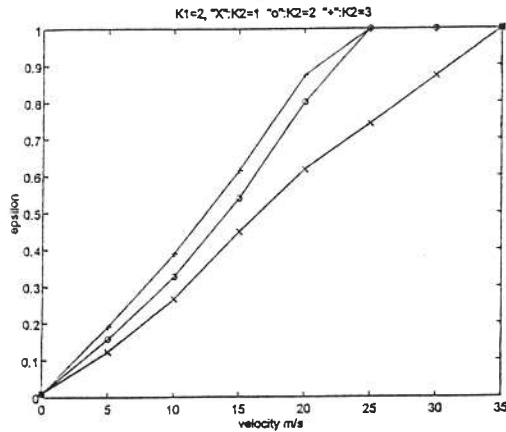


Figure 7 : translational mode,  $\xi$  as a function of  $U_a^*$  and as a function of  $K_1$  and  $K_2$

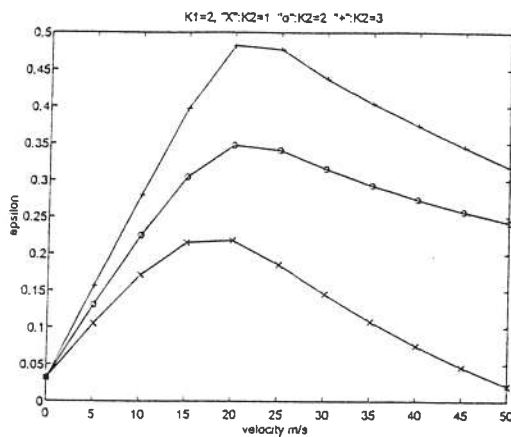


Figure 8 : rotational mode,  $\xi$  as a function of  $U_a^*$  and as a function of  $K_1$  and  $K_2$

The translational mode is fluidelastically stable : if the velocity increases the reduced damping increases, even if  $K_1 > K_2$ . The reduced damping evolutions are close to the ones obtained for only downstream pressure losses (Figure 5) :

\* the stability of the translational mode is not affected by the upstream pressure losses.

The reduced damping of the rotational mode drops to the negative : the system becomes unstable at velocities higher than 50m/s, even if  $K_2 > K_1$ . Note that the drops are not as abrupt as the ones obtained for only upstream pressure loss (Figure 3), if the downstream pressure loss factor increases, the drop decreases :

\* the upstream pressure losses cause the system to flutter, while the downstream pressure losses stabilize it, but the negative damping has stronger effects than the positive damping.

### CONCLUSION

An iterative method has been developed to perform a stability predictive analysis of a flow channel. This method used the fluidelastic force obtained with the "linearizing-of pressure-losses" model. This force was written, by Porcher (1994), for several boundary conditions. Three of them have been studied.

The parametric study shows that :

\* the structure is stable for only downstream pressure losses (positive damping),

\* the structure is unstable for only upstream pressure losses (negative damping),

- if the flow velocity increases, a flutter instability affects the two modes,

- if the pressure loss factor increases, the critical velocity decreases,

\* the structure is unstable, for one mode, for both upstream and downstream pressure losses,

- if the flow velocity increases, the reduced damping of the rotational mode drops to the negative,

- if the downstream pressure loss factor increases, the drop decreases.

The "linearizing-of pressure-losses" model is able to predict the negative damping mechanism, which causes the structure to flutter, and the positive damping mechanism, which stabilizes it. This study has shown that the negative damping has stronger effects than the positive damping on the stability of the structure.

Pressure loss factor $K_1$	1	2	3
Translational mode, critical velocity (m/s)	26	20	17
Rotational mode, critical velocity (m/s)	48	37	31

Table 3 : critical velocities

Note that :

- \* the critical velocity, which causes the system to flutter, decreases when the pressure loss factor increases,
- \* the flow velocity required for instability for the translational mode is higher than that for the rotational mode : the translational mode becomes unstable before the rotational mode.

These results agree with the stability analysis performed by Porcher (1994), in which only the diagonal terms of the matrix  $[A_a(\omega)]$  were considered. But, in this study, the flutter instability was found to first affect the rotational mode. An analytical investigation revealed that this difference can be explained by the nondiagonal terms of the matrix  $[A_a(\omega)]$  which increase more rapidly than the diagonal terms. For the translational mode, Figure 4 shows that the matrix coefficient  $A_a(1, 2)$  strongly increases if  $U_a^*$  increases. In this case, the stability of the structure is first affected by this term.

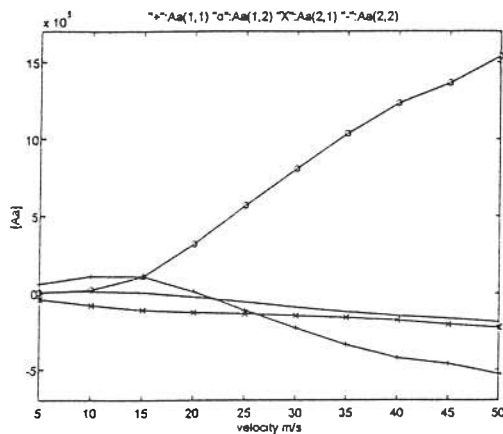


Figure 4 : translational mode,  $K_1=2$ ,  $A_a(i, j)$  as a function of  $U_a^*$

### Downstream pressure loss

The dependance of  $\xi$  upon  $U_a^*$  and upon the downstream pressure loss factor  $K_2$  is shown on Figure 5 for the translational mode and on Figure 6 for the rotational mode.

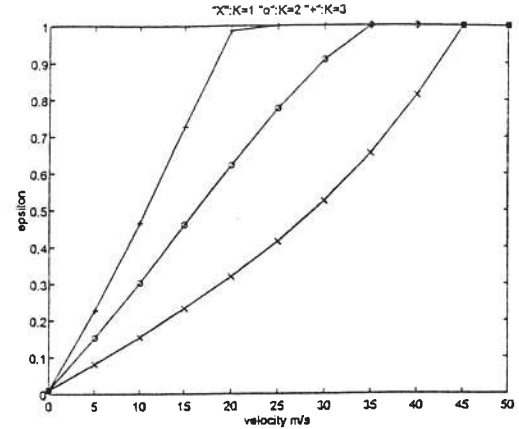


Figure 5 : translational mode,  $\xi$  as a function of  $U_a^*$  and as a function of  $K_2$

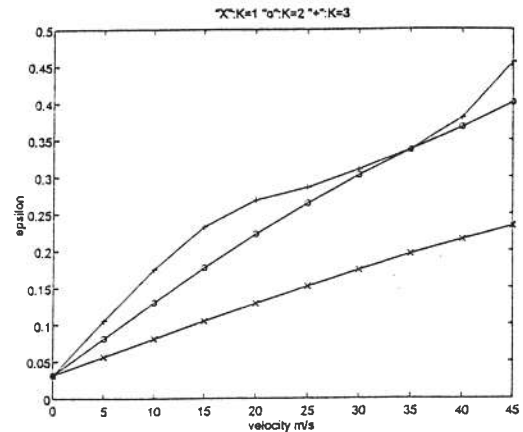


Figure 6 : rotational mode,  $\xi$  as a function of  $U_a^*$  and as a function of  $K_2$

Note that :

- \* at a given value of  $K_2$ , increasing the velocity increases the reduced damping. The two modes are fluidelastically stable. A positive damping mechanism stabilizes the system. (On Figure 5, reduced dampings equal to 100% are obtained! These results, which have no physical sense, are due to the relation (5) : if  $\omega$  has no real part,  $\xi = 1$ ),
- \* at a given value of  $U_a^*$ , the damping ratio,  $\xi$ , increases if the pressure loss factor,  $K_2$ , increases,
- \* at a same velocity the structure is stable for downstream pressure losses, while it is unstable for upstream pressure losses.

## REFERENCES

De Langre, E., Granger, S., 1995, "Couplage Structure-Ecoulement Axial Confiné", *Revue Française de Mécanique*, Vol 1995-1, pp49-55.

De Langre, E., Bélanger, F., Porcher, G., 1990, "Linearized Potential Flow Theory Applied to Calculation of Fluidelastic Forces in Annular Flow Configurations", *ASME/JSME/I.Mech.E/IAHR 3rd International Symposium on Flow-Induced Vibration and Noise*, Vol.5, pp.187-204, Anaheim, California.

Inada, F., Hayama, S., 1988, "A Study Leakage-Flow-Induced Vibrations (Fluid-Dynamic Forces Acting on the Walls of a One-Dimensional, Narrow Passage)", *JSME International Journal*, Vol.31, pp.39-47.

Inada, F., Hayama, S., 1988, "A study on Leakage-Flow-Induced Vibrations. Part.II : Stability Analysis and Experiments for Two-Degree-of-Freedom Systems Combining Translational and Rotational Motions", *Journal of Fluids and Structures*, Vol.4, pp.413-428.

Mateescu, D., Païdoussis, M.P., 1985, "The Unsteady Potential Flow in an Axially Variable Annulus and its Effect on the Dynamics of the Oscillating Rigid Center-Body", *Journal of Fluids Engineering*, September 1985, Vol.107, pp.421-427.

Miller, D.R., 1970, "Generation of positive and negative damping with a flow restrictor in axial flow", *Proceedings of the Conference on Flow-Induced Vibrations in Reactor System Components*, May 14-15, 1970, pp.304-307.

Mulcahy, T.M., 1988, "One-Dimensional Leakage-Flow Vibration Instabilities", *Journal of Fluids and Structures*, Vol.2, pp.383-403.

Païdoussis, M.P., 1966, "Dynamics of Flexible Slender Cylinders in Axial Flow, Part I : Theory, Part II : Experiments", *Journal Fluid Mechanics*, Vol.26, Part 4, pp.717-751.

Porcher, G., 1994, "Contribution à l'étude des instabilités fluide élastiques de structures tubulaires sous écoulement axial confiné", Thesis, University Paris VI.

Porcher, G., De Langre, E., 1995, "Fluidelastic instability in a confined annular flow : an experimental and analytical approach", *ASME/PVP/ICPVT-8 Conference, Symposium on flow-induced vibrations*, 1996 July 21-26, Montreal, Quebec.

Spurr, A., Hobson, D.E., 1984, "Forces on the Vibrating Centrebody of an Annular Diffuser", *The ASME Winter Annual Meeting New Orleans*, 9-14 December 1984, Louisiana, Symposium on Flow-Induced Vibrations, Vol.4, Vibration Induced by Axial and Annular Flows, pp.41-52.

## APPENDIX

### The dimensionless variables

The variables are rendered non-dimensionnall by using the following notations :

$$X = \frac{X^*}{L^*} ; U = \frac{U^*}{U_a^*} ; \omega = \frac{L^* \omega^*}{U_a^*}$$

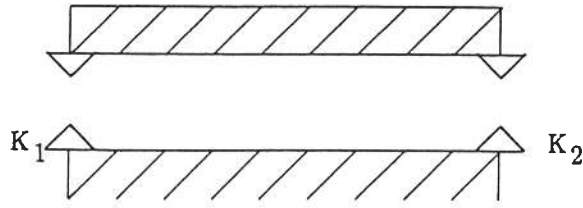
where  $L^*$  is the half length of the structure and  $U_a^*$  is the upstream velocity.

### The structural matrix

Structural Matrix	dimensionless form
$[M_s]$	$\frac{1}{\rho L^{*2}} \begin{bmatrix} m^* & 0 \\ 0 & \frac{m^*}{3} \end{bmatrix}$
$[A_s]$	$\frac{1}{\rho L^* U_a^*} \begin{bmatrix} C_1^* + C_2^* & C_2^* - C_1^* \\ C_2^* - C_1^* & C_1^* + C_2^* \end{bmatrix}$
$[R_s]$	$\frac{1}{\rho U_a^{*2}} \begin{bmatrix} k_1^* + k_2^* & k_2^* - k_1^* \\ k_2^* - k_1^* & k_1^* + k_2^* \end{bmatrix}$

Table 1 : structural matrix

**The fluidelastic force**



$$F = \{ \omega^2 [M_a] - i\omega [A_a(\omega)] - [R_a(\omega)] \} \begin{pmatrix} X_G \\ \theta \end{pmatrix}$$

Dimensionless Matrix	
$[M_a]$	
$\begin{bmatrix} \frac{2}{3} \epsilon & 0 \\ 0 & \frac{2}{45} \epsilon \end{bmatrix}$	
$[A_a(\omega)]$	
$\begin{bmatrix} \frac{\epsilon [2\omega^2 + 2\bar{K}_1 \bar{K}_2 + \bar{K}_2 - \bar{K}_1] (\bar{K}_1 + \bar{K}_2)}{4\omega^2 + (\bar{K}_1 + \bar{K}_2)^2} & \frac{2\epsilon [4\omega^2 + (\bar{K}_1 + \bar{K}_2)^2 + (\bar{K}_2 - \bar{K}_1)(2\omega^2 - 6) + 4(\bar{K}_1^2 + \bar{K}_2^2 - \bar{K}_1 \bar{K}_2)]}{3 [4\omega^2 + (\bar{K}_1 + \bar{K}_2)^2]} \\ - \frac{2\epsilon [4\omega^2 + (\bar{K}_1 + \bar{K}_2)^2 + 2\omega^2 (\bar{K}_1 - \bar{K}_2)]}{3 [4\omega^2 + (\bar{K}_1 + \bar{K}_2)^2]} & \frac{2\epsilon (\bar{K}_1 + \bar{K}_2) [2\omega^2 - 3(\bar{K}_1 - \bar{K}_2)]}{9 [4\omega^2 + (\bar{K}_1 + \bar{K}_2)^2]} \end{bmatrix}$	
$[R_a(\omega)]$	
$\begin{bmatrix} - \frac{2\epsilon (\bar{K}_1 - \bar{K}_2) (\bar{K}_1 - \bar{K}_2 + 2)\omega^2}{4\omega^2 + (\bar{K}_1 + \bar{K}_2)^2} & \frac{2\epsilon (\bar{K}_1 + \bar{K}_2) [(\bar{K}_1 - \bar{K}_2 + 8)\omega^2 + 3(\bar{K}_2 - \bar{K}_1 + 2\bar{K}_1 \bar{K}_2)]}{3 [4\omega^2 + (\bar{K}_1 + \bar{K}_2)^2]} \\ \frac{2\epsilon (\bar{K}_1^2 - \bar{K}_2^2)\omega^2}{3 [4\omega^2 + (\bar{K}_1 + \bar{K}_2)^2]} & - \frac{2\epsilon [(\bar{K}_1 + \bar{K}_2)^2 (\omega^2 + 3) + 6(\bar{K}_1 - \bar{K}_2 + 2)\omega^2]}{9 [4\omega^2 + (\bar{K}_1 + \bar{K}_2)^2]} \end{bmatrix}$	

Table 2 : the fluidelastic-force matrix for upstream and downstream pressure losses with no friction through the fluid area